The Influence of Carbon Black Batches on the Fracture Behavior of Glass Fiber Reinforced PA6/PA66 Blends

Markus Kroll,[1] Beate Langer,[2] Siegfried Schumacher,[1] Wolfgang Grellmann[2,3]

[1]*BASF Leuna GmbH, Leuna D-06237, Germany*
[2]*Polymer Service GmbH Merseburg, Merseburg D-06217, Germany*
[3]*Center of Engineering Sciences, Martin-Luther-University Halle-Wittenberg, Halle/Saale D-06099, Germany*

Received 22 July 2009; accepted 11 October 2009
DOI 10.1002/app.31611
Published online 1 December 2009 in Wiley InterScience (www.interscience.wiley.com).

ABSTRACT: The toughness behavior of 30 wt % glass fiber reinforced PA6/PA66 blends colored with different masterbatches containing carbon black (CB) was characterized by the instrumented Charpy impact test. Two different CB types with different particle diameters as well as two different polymers, PE and PA6, were used to prepare the masterbatches. The CB concentration was varied from 0 to 1.2 wt % in the compounds and all materials were examined dry and after water absorption. The toughness of the compounds significantly decreased when CB was incorporated. Moisture conditioning of the materials led to increased toughness and ductility but did not compensate for the negative influence of CB. Using PE as a masterbatch polymer succeeded in limiting the influence of CB on toughness whereas the largest particle diameter led to the highest reduction in toughness. By taking into account crack resistance curves, it could be shown that there is a significant change in crack propagation behavior when the concentration of the larger particle CB exceeds a certain level; this was ascribed to the existence of complex CB structures at this concentration. © 2009 Wiley Periodicals, Inc. J Appl Polym Sci 116: 610–618, 2010

Key words: polyamides; fracture; reinforcement; toughness; dyes/pigments

INTRODUCTION

Glass fiber reinforced PA6/PA66 blends are used for several applications, especially in the automotive industry. The combination of the good processability and higher surface quality of Polyamide 6 with the enhanced temperature resistance of Polyamide 66 leads to application-specific compounds, primarily for visible parts or assemblies within engine bays or interiors. Blending PA6 and PA66, the influence of the relationship between the mass fractions of these two miscible components as well as the influence of an additional inhibition of a toughening modifier are well described in the literature.[1–3] The blend properties are frequently compared to the properties of *in situ* polymerized PA6/PA66 composites, where the molecular composites often provide very specific characteristics and relatively high effects at very low PA66 mass fraction levels.[4–6] For the present study, a 50/50 blend of PA6 and PA66 was used and was compounded with 30 wt % of glass fibers and different carbon black (CB) batches.

CB pigments are commonly used for coloring. The use of CB as a coloring pigment also provides a protection against UV-radiation which makes it an ideal candidate for the pigmentation of automotive parts. Generally, the presence of CB leads to a reduction in mechanical properties such as elongation at break or impact toughness whereas material stiffness is increased.[7–11] In comparison to other available polyamide colorants such as spinel or iron oxide, CB provides higher strength and hardness values.[1] There are several reasons for property changes with increasing CB concentration. First of all, the CB acts as a nucleating agent and leads to changes in the crystallization temperature as well as in the size and structure of the resulting crystallites, especially when used in low concentrations as is usual for color pigmentation.[12,13] Furthermore, CB has a positive effect on the melt flow rate (MFR) and this leads, especially in glass fiber reinforced polyamides, to increased strength and stiffness.[10,14]

Besides crystallization and melt processing, the pigments directly influence the morphology of the polymer compound.[7] On the one hand, CB claims up to 6 times its own volume in the compound, which leads to a significant reduction in the free matrix volume and a decrease in the compound's plastic deformation capability. On the other hand, the dispersion of this particle filler is inhomogeneous because of local variations in the matrix morphology. Moreover, the CB tends to build up agglomerates as well as whole networks in higher CB concentrations, which influence the compound morphology.[7] All these morphological changes also

Correspondence to: M. Kroll (markus.kroll@basf.com).
Contract grant sponsor: BASF Leuna GmbH.

TABLE I
CB Batch Compositions, MFR and Moisture Content of the Analyzed Materials

PA6/PA66 (50/50) + 30 wt % short glass fibers					
Batch type			Melt flow	Moisture content	
Batch matrix polymer	CB particle diameter (nm)	CB content compound (wt %)	MFR (g/10 min)	Dry (%)	Conditioned (%)
	Uncolored		14.8	0.05	2.11
PA6	16	0.3	17.0	0.06	2.08
PA6	16	0.6	16.6	0.05	2.11
PA6	16	1.2	18.0	0.05	2.10
PA6	47	0.3	18.1	0.04	2.05
PA6	47	0.6	16.7	0.05	2.03
PA6	47	1.2	15.8	0.05	1.98
PE	16	0.3	18.7	0.06	2.15
PE	16	0.6	20.0	0.05	1.96
PE	16	1.2	19.7	0.07	1.98

lead to increased stiffness and strength in addition to reduced elongation at break and toughness respectively.

There are several CB types available for compounding applications. These types differ according to their fabrication in terms of structure and properties, with primary particle sizes between 10 and 500 nm, specific surface areas between 10 and 1000 m^2/g and a diverse tendency to develop aggregates and agglomerates.[15–17]

The process of water absorption[18–21] as well as the influence of chemically bonded and dissolved water on viscoelastic and mechanical properties have been intensively investigated for many different polyamide materials.[22–25] The influence of water on the toughness behavior of polyamides is a topic that has been analyzed also by using fracture mechanical procedures.[26]

The influence of CB on the thermal, rheological and mechanical properties of polyamides is well documented in the literature whereas there is still a need to examine the changes in fracture mechanical properties with different CB batch types and concentrations, especially where the CB content is very low as is usual for compound coloring. The influence of the CB pigment size and the batch matrix polymer type on the mechanical properties and the resistance against unstable crack propagation in a fracture mechanical approach were investigated in this study. Furthermore, changes in the material properties of these colored glass fiber reinforced PA6/PA66 blends after moisture absorption were examined.

EXPERIMENTAL

Materials

Composition

Glass fiber reinforced PA6/PA66 blends were produced on a corotating twin screw extrusion machine. The granulate was dried in a condensation dryer at 80°C for 24 h after extrusion to reach a moisture content of about 0.05%. The specimens were produced on an injection molding machine and subsequently stored at 0% relative humidity. To provide additional information concerning the material properties in a normal conditioned state, specimens of each material were stored in a climate chamber at 70°C and 62% relative humidity until the moisture equilibrium had established according to ISO 1110.[27]

Three different batches were used to provide the CB pigments. The compositions and the batch components of the ten analyzed materials together with the MFR of granulates (according to ISO 1133[28]) and the compound moisture content of the specimens after conditioning are given in Table I. The present moisture content of the compounds almost exactly fits the known moisture concentrations of the neat polyamide blends at equilibrium, reduced by the mass fraction of glass fibers, CB and PE. This proves that there is no significant incident of water transport or absorption processes caused by the fillers.

Influence of moisture absorption

Water absorption of about 2% of the specimen's mass leads to a change in viscoelastic properties. This could be revealed by dynamic mechanical thermal analysis (DMTA). The influence of water content on the glass transition temperatures of the uncolored compound and the compounds with a medium CB concentration is shown in Table II. Normal conditioning induces a reduction in T_g of about 40 K.

The brittle behavior of the dry materials at room temperature is changed into a more ductile material behavior through the influence of water in the amorphous regions of the compounds. The polyamide

TABLE II
Glass Transition Temperatures Determined in DMTA as the Maximum of tan δ of Dry and Conditioned Compounds

Batch (CB content = 0.6 wt %)	DMTA T_g dry (°C)	DMTA T_g conditioned (°C)	ΔT_g (K)
Uncolored	58.0	17.0	−41.0
PA6/CB (16 nm)	59.3	22.3	−37.0
PA6/CB (47 nm)	58.0	19.5	−38.5
PE/CB (16 nm)	56.4	20.1	−36.3

matrix is plasticized by the bonded water molecules, which leads to a rising fraction of plastic deformation and yielding under tensile load, for example, as is presented in Figure 1.

Basic characterization

To characterize the crystallization and melting behavior, differential scanning calorimetry (DSC) according to ISO 11,357[29,30] was used. For further investigation of the glass transition temperature T_g, DMTA pursuant to ISO 6721-1[31] was carried out to observe changes in rising moisture content. Mechanical properties under quasi-static load were analyzed in tensile tests according to ISO 527.[32,33] To achieve a basic toughness characterization of the polyamide compounds, Charpy notched impact tests were performed in accordance with ISO 179-1.[34]

Fracture mechanical characterization

Conventional toughness characterization using the Charpy impact test was complemented by a fracture mechanical investigation using the instrumented Charpy impact test (ICIT). The standard used was the "procedure for determining the crack resistance behavior by ICIT"[35] that was developed at the Institute of Materials Science at the Martin-Luther-University Halle-Wittenberg.

Following this procedure, the unstable and stable crack growth behavior of the compound materials was analyzed. Therefore, single-edge notched bend (SENB) specimens with the dimensions 4 × 10 × 80 mm^3 ($B \times W \times L$) were used.

For the characterization of the unstable crack growth behavior, the initial crack a had a length of 2 mm resulting in an a/W ratio of 0.2 and was cut with a metal blade with an edge sharpness of 0.3 μm. As a characteristic value of linear elastic fracture mechanics, the fracture toughness T_g can be determined by eq. (1).

$$K_{\mathrm{Id}} = \frac{F_{\max} s}{B W^{3/2}} f\left(\frac{a}{W}\right) \tag{1}$$

W is the specimen width and B the sspecimen thickness, a is the initial length of the crack, $F_{\max}$ is the maximum load measured in the ICIT, s is the width between the supports and $f(a/W)$ is a geometric function. The critical crack tip opening displacement (CTOD) δ_{Id} can be calculated according to eq. (2).

$$\delta_{\mathrm{Id}} = \frac{1}{n}(W - a)\frac{4 f_{\max}}{s} \tag{2}$$

Here $f_{\max}$ is the deflection at maximum load $F_{\max}$ and n is the rotational factor of the plastic hinge model.[35,36]

The characteristic value J_{Id} was calculated according to the J-integral estimation method of SUMPTER and TURNER given in eq. (3), where the total deformation energy is divided into an elastic part A_{el} and a plastic part A_{pl}. The notch depth influence is represented by the geometric functions η_{el} and η_{pl} and the effective crack length by a_{eff}.[35]

$$J_{\mathrm{Id}} = \eta_{\mathrm{el}} \frac{A_{\mathrm{el}}}{B(W-a)} + \eta_{\mathrm{pl}} \frac{A_{\mathrm{pl}}}{B(W-a)} \frac{W - a_{\mathrm{eff}}}{W - a} \tag{3}$$

For a profound characterization of the crack growth behavior of the compounds, the stable crack propagation process was analyzed using the second part of the procedure described in.[35] In a multi-specimen experiment, a stop block was used to realize different crack propagations and to record crack resistance curves (R-curves) as they are known in the literature.[35,36] For each material, several SENB specimens with an initial crack length of 4.5 mm and a notch sharpness of 0.3 μm were used. By deploying the stop block as a device for halting the pendulum, different deflections were realized and a load-

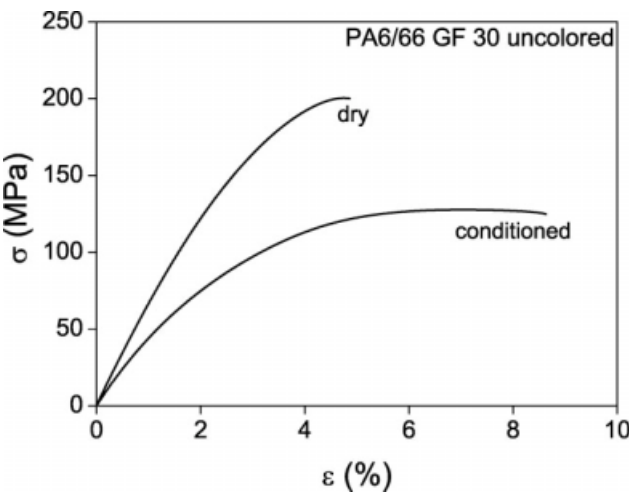

Figure 1 Stress–strain curves of dry and conditioned uncolored 30 wt % reinforced PA6/PA66 blends from tensile test.

TABLE III
Mechanical Properties of Compounds with Different CB Contents

Batch: PA6/CB (47 nm) CB content (wt %)	Tensile test			Charpy notched impact test
	E_t (MPa)	σ_m (MPa)	ε_B (%)	a_{cN} (kJ/m^2)
Dry				
0 uncolored	9670	201	4.3	13.1
0.3	9370	175	3.4	7.3
0.6	9430	170	3.3	7.0
1.2	9720	174	3.3	6.2
Conditioned				
0 uncolored	5610	128	7.7	22.7
0.3	5510	106	7.0	13.5
0.6	5660	107	6.7	12.1
1.2	5630	104	6.7	11.1

deflection diagram for each specimen was recorded. Each deflection results in a different length of stable crack growth Δa, which has to be measured before building up the R-curve from the pairs of J_I values of each diagram and the corresponding Δa.

This method is not appropriate when highly reinforced materials are investigated, because the measurement of Δa is complicated by the roughness of fracture surfaces of reinforced materials. Different methods to gain R-curves can be found in the literature.[1,37,38]

In this study, the characteristic fracture mechanical parameter J_I was related to the fracture time t_F of each specimen.[39]

RESULTS AND DISCUSSION

Influence of the CB weight fraction

Basic characterization

In Table III, the mechanical properties of the compounds with different weight fractions of 47 nm CB are shown. Both strength and elongation at break drop significantly when CB is present and these characteristics remain constant in a dry state as well as in a conditioned state when the CB concentration is increased. The Young's modulus tends to decrease at low CB concentrations in a dry state but recovers at 1.2 wt %. In contrast to this moderate behavior, under tensile load the impact toughness of the compounds decreases dramatically by about 50% already at the lowest CB concentration and decreases further with rising CB content.

Fracture mechanical characterization

Load-deflection diagrams of the ICIT were analyzed. In Figure 2, the load-deflection diagrams of the dry and conditioned compounds are illustrated. The overall shape of the recorded load-deflection curve is predominantly influenced by the water content. While the dry specimens show ideal elastic behavior, the conditioned specimens are characterized by an elastic-plastic deformation and a characteristic F_{gy}.

A very high deflection f_{max} at maximum load F_{max} is characteristic of conditioned specimens. With the

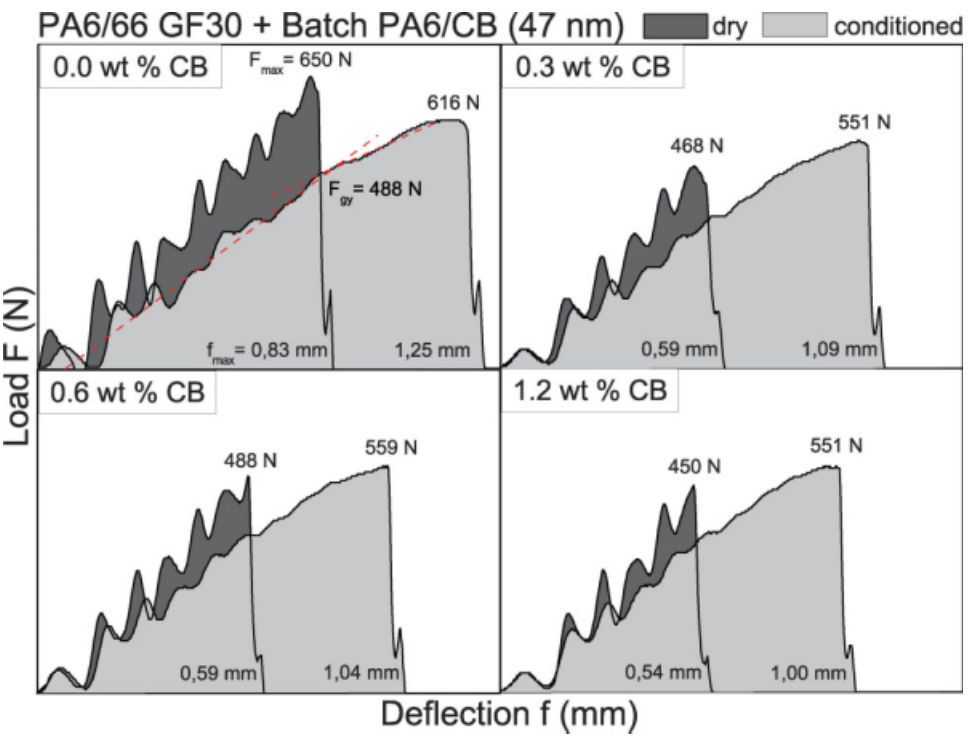

Figure 2 Load-deflection diagrams of PA6/66 GF30 with different concentrations of 47 nm CB. [Color figure can be viewed in the online issue, which is available at www.interscience.wiley.com.]

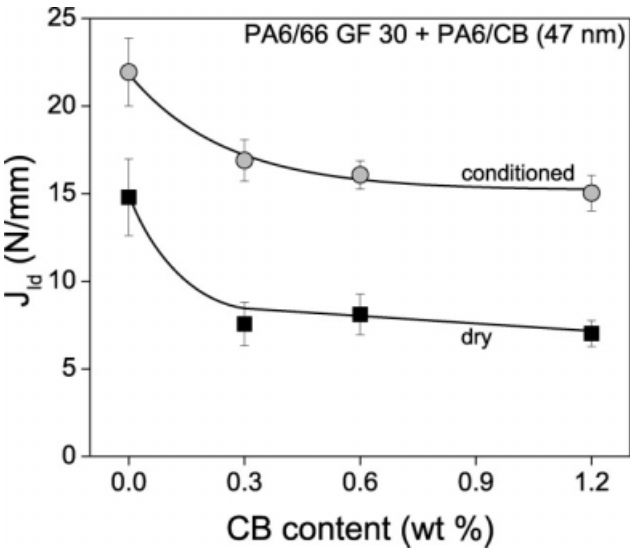

Figure 3 Influence of CB content on the resistance against unstable crack growth J_{Id}.

influence of water, the different CB content dramatically affects the shape of the curves, the maximum loads and deflections. With rising CB content, the maximum deflections decrease. In contrast to this, the maximum load drops with the presence of CB and subsequently remains relatively constant. This behavior corresponds to the change in strength and stiffness in Table III. Due to the fact that CB acts as a deformation inhibiting particle, the constant loss of toughness with rising CB concentration can be ascribed to the reduction in the deformation capability of the material caused by the CB itself and the bound matrix volume, as was mentioned by Wessling.[7]

The influence of CB content on the parameter J_{Id} is illustrated in Figure 3. Here the amount of linear elastic and elastic-plastic deformation energy is taken into account. The resistance against unstable crack growth J_{Id} is increased by about 50% by the influence of water in the case of the uncolored compound and by about 100% in the case of CB filling. Water absorption significantly increased the deformation energy. The reason can be found in the fact that water molecules, when they replace hydrogen bonding, lead to a reduction in the glass transition temperature from about 60°C to a value around room temperature (see Table II) and are responsible for a plastification of polyamides.[18] This leads to the enhancement of the resistance against unstable crack propagation in unreinforced PA.[26]

The J-value decreased with the presence of CB. This effect was found both in dry and in conditioned specimen states. The change from linear elastic to elastic-plastic deformation induced by the moisture content could be revealed by scanning electron microscopy (SEM). In Figure 4, the fracture surfaces of the SENB specimens of the compounds without any batch and with 0.6 wt % of the batch PA6/CB (47 nm) are compared. The razor blade notch is located

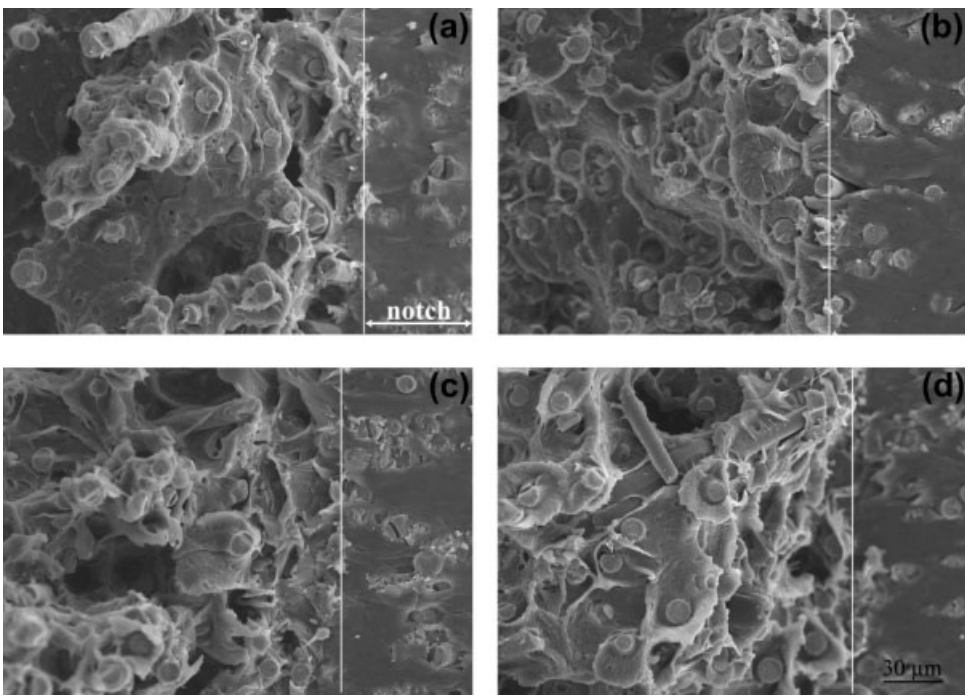

Figure 4 Fracture surfaces of PA6/66 GF30 compounds: (a) uncolored dry, (b) 0.6 wt % PA6/CB (47 nm) dry, (c) uncolored conditioned, (d) 0.6 wt % PA6/CB (47 nm) conditioned (the white line marks the edge of the razor blade notch on the right-hand side).

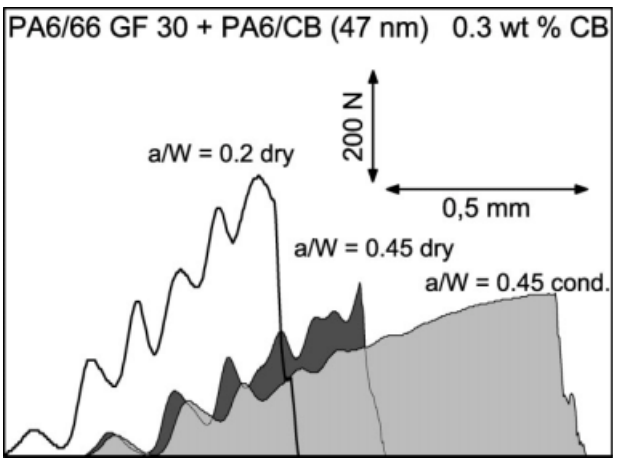

Figure 5 Load-deflection diagrams of PA6/66 GF30 PA6/CB (47 nm) with 0.3 wt % CB and different *a/W* ratios.

on the right-hand side of each picture (smooth with cut glass fibers). On the left-hand side, the fracture surface is apparent. The matrix of the uncolored compound is characterized by many microscopic holes and cavities in a dry state [Fig. 4(a)] whereas the matrix of the compound containing CB in [Fig. 4(b)] shows fewer holes. Generally, the matrix appears much more brittle in [Fig. 4(b)] whereas there are indications of small plastic deformations in [Fig. 4(a)] such as torn matrix segments and fibrils.

After conditioning, both compounds show large amounts of plastic deformation in Figure 4(c,d), nonetheless the uncolored compound is characterized by a superior level of cavitation which is the explanation for the change in the *J*-value. Therefore, the inhibition of plastic deformations through using CB could be evidenced.

The amount of stable crack propagation before initiation of unstable crack growth could be increased by adjusting the specimen geometry and the experimental conditions. The change in the fracture process is represented by the shift to larger elastic-plastic deformation fractions in the load-deflection diagrams of the specimens with an *a/W* ratio of 0.45 in Figure 5.

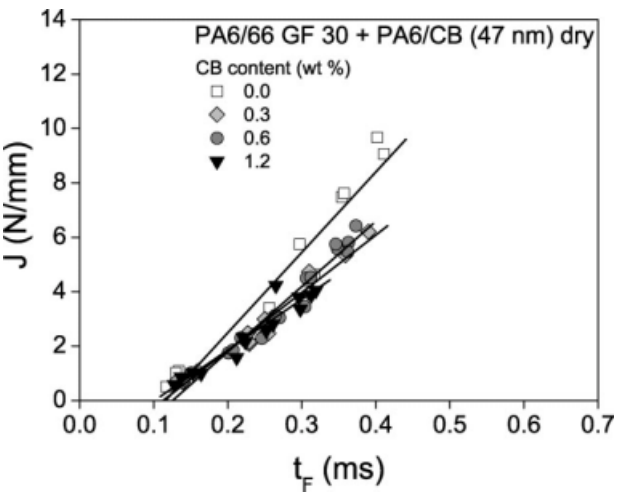

Figure 6 $J - t_F$ curves of PA6/66 GF30 with batch PA6/CB (47 nm) in a dry state.

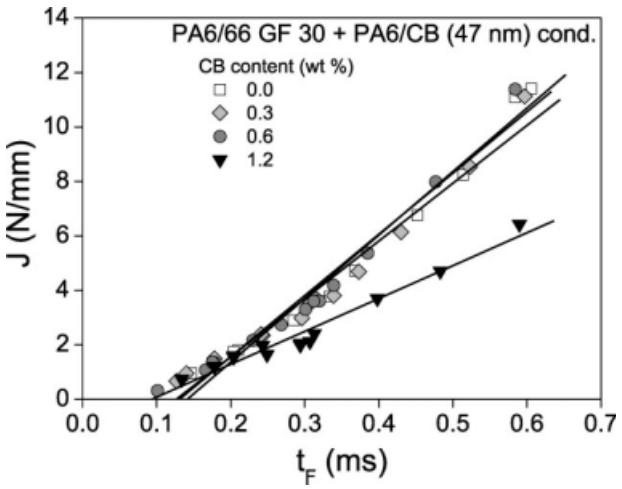

Figure 7 $J - t_F$ curves of PA6/66 GF30 with batch PA6/CB (47 nm) in a conditioned state.

As a result, the stable crack propagation could be characterized by J–t_F curves in Figures 6 and 7. The capability of the material to dissipate energy during stable crack propagation is reduced by the CB. There is less energy dissipation per time and the slope of the J–t_F curve continuously decreases with rising CB content in a dry state. The conditioned PA compounds show another behavior. Here the water induced plastification of the matrix leads to a reduction in the negative CB influence on the dissipated energy per time (dJ/dt_F) up to 0.6 wt % CB. At 1.2 wt % CB, there is a dramatic decrease in the slope of the curve. But also the total time for fracture is nearly twice as high in the conditioned material

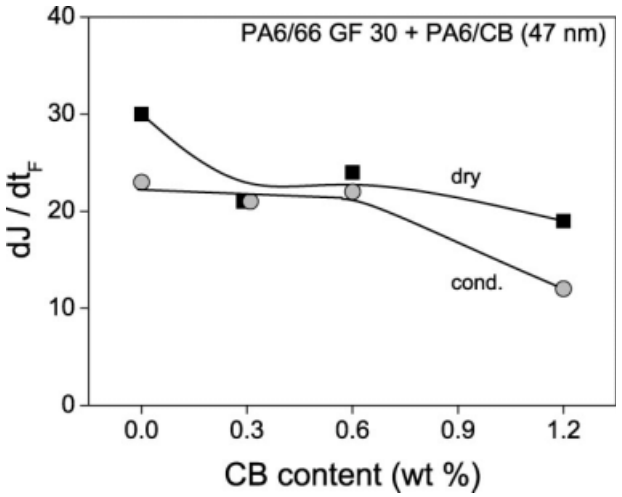

Figure 8 Slopes of $J - t_F$ curves of PA6/66 GF30 with batch PA6/CB (47 nm).

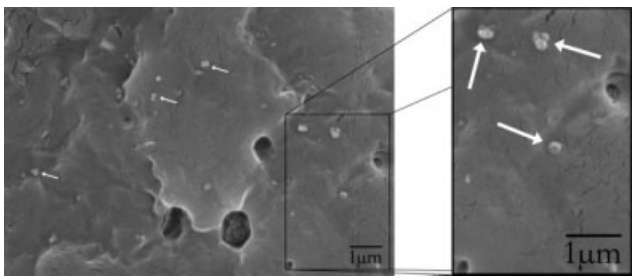

Figure 9 Fracture surface of PA6/66 GF 30 + PA6/CB (47 nm) with 1.2 wt % CB (white arrows mark CB structures).

(dry: 0.3–0.4 ms; wet: 0.6 ms) so that the total energy dissipation during stable crack propagation is higher.

These different behaviors in dry and conditioned states are illustrated in Figure 8. The CB influence is already significant at 0.3 wt % in a dry state whereas the value dJ/dt_F is nearly constant from 0 to 0.6 wt % CB in a conditioned state. The drop of the slope at 1.2 wt % CB was present before and after conditioning but more significant in the conditioned material.

The structure development of CB is characterized by sudden changes at characteristic points such as the percolation threshold when the concentration increases.[7] The morphological difference between the compounds with 0.3 or 0.6 wt % CB (47 nm) and 1.2 wt % CB was identified in SEM. While there were no visible CB structures on the fracture surfaces of the compounds with low CB concentration, the SEM image of PA6/66 GF30 + PA6/CB (47 nm) with 1.2 wt % CB in Figure 9 shows the existence of complex CB structures in a size range between 100 and 300 nm (see white arrows). These CB structures seem to build up in larger numbers as soon as the concentration of CB exceeds a certain level and therefore are supposedly responsible for the sudden drop of the slope of the R-curves (Fig. 7) as they support the crack growth.

Influence of the batch polymer and the CB particle size

Basic characterization

In Table IV, the mechanical and thermal properties of those compounds with the 0.6 wt % CB are compared with the uncolored reference. Regardless of which batch was used, the presence of CB always leads to a decrease in strength and toughness whereas stiffness is slightly increased when PA6 was the batch base polymer.

Besides the influence of enhanced melt flow and the structural influence of CB as a rigid filling particle, the nucleation effect of these nanoscaled structures leads to a change in the crystallite size and structure which could be proved by the rise of peak crystallization temperatures T_{pc} when CB was introduced. In this study, the smallest CB particles with a diameter of 16 nm lead to the highest increase in T_{pc}. When the particle diameter is increased, the nucleation effect declines and the crystallization temperature is only slightly above T_{pc} of the uncolored material.

Comparing the batch on the base of polyethylene with that on the base of polyamide and the same particle diameter, the lower crystallization temperature of the compound with the PE batch suggests a lower nucleation effect. That could be ascribed to the fact that immiscible blends such as PA/PE build up a certain CB distribution structure depending on the order of CB incorporation and on the viscosity differences between the polymers.[40] So, both the concentration and the distribution of CB should differ between the polyamide phases of the two compounds, with the tendency of a lower concentration or more irregular distribution of CB in the PA phase of the compound with PE as a batch polymer.

Fracture mechanical characterization

Table V gives a good overview of the characteristics of the ICIT that determine the fracture behavior of the compounds. The batch PE/CB (16 nm) provides the highest fracture toughness K_{Id} in a dry state and the batch PA/CB (16 nm) the highest fracture toughness in a conditioned state. While the fracture toughness of the compounds with the 16 nm CB batches (PE and PA6) decreased after conditioning, K_{Id} increased in the case of PA6/CB (47 nm). K_{Id} is a load-determined characteristic, therefore the reduction in the maximum load by conditioning the compounds with the small diameter CB (compare Fig. 2)

TABLE IV
Mechanical and Thermal Properties of Compounds with Different CB Batches

	Tensile test		DSC		Charpy notched impact test
Batch (CB content = 0.6 wt %, dry)	E_t (MPa)	σ_m (MPa)	T_{pc} PA6 (°C)	T_{pc} PA66 (°C)	a_{cN} (kJ/m^2)
Uncolored	9670	201	194	219	13.1
PA6/CB (16 nm)	9950	191	192	224	9.4
PA6/CB (47 nm)	9720	174	193	221	6.2
PE/CB (16 nm)	9550	179	192	222	10.4

TABLE V
Fracture Mechanical Characteristics from ICIT of Compounds with Different CB Batches

Batch (CB content = 0.6 wt %)	ICIT		
	K_{Id} (MPa mm$^{1/2}$)	δ_{Id} (10^{-3} mm)	J_{Id} (N/mm)
Dry			
PA6/CB (16 nm)	230.1	137	11.1
PA6/CB (47 nm)	195.9	113	8.1
PE/CB (16 nm)	237.1	140	11.9
Conditioned			
PA6/CB (16 nm)	229.1	220	19.0
PA6/CB (47 nm)	214.9	203	16.1
PE/CB (16 nm)	222.6	214	18.0

led to reduced fracture toughness. When 47 nm CB was incorporated, the maximum load and K_{Id} were significantly lower than in the other cases in a dry state. In this case, conditioning led to a rise in maximum load and K_{Id}. The deformation determined CTOD δ_{Id} increased dramatically after conditioning in each compound because of the strong deformation increase. J_{Id} as an energy determined characteristic also increases after conditioning. The use of 47 nm CB leads to the lowest fracture toughness K_{Id}, the lowest CTOD δ_{Id} and the lowest *J*-value, both dry and conditioned, and should therefore be avoided as a coloring pigment for toughness-sensitive applications.

The influence of the CB content on the *J*-value of the three different batches is illustrated in Figure 10. While the smaller CB particle diameter generally provides a higher crack resistance, the polyethylene does additionally enhance toughness and tends to compensate for the negative influence of CB at higher concentrations. The amount of the batch polymer in the compound is defined through the concentration of CB. That means that the batch matrix polymer content in the compound with 1.2% CB is twice as high as in the compound with 0.6% CB.

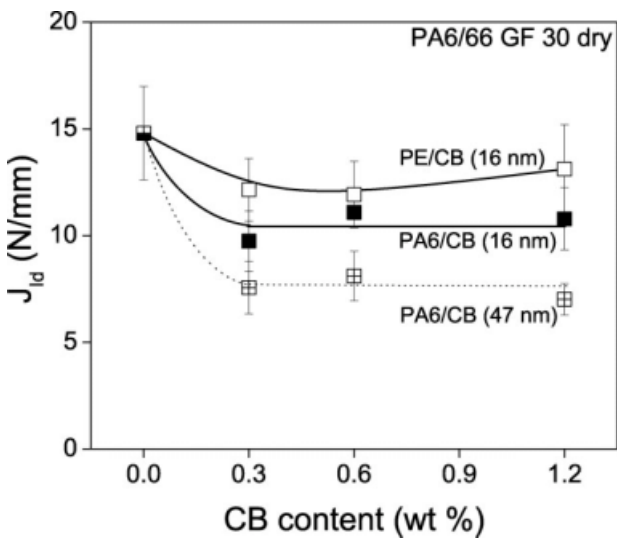

Figure 10 Influence of the CB content and the batch type on the resistance against unstable crack growth J_{Id}.

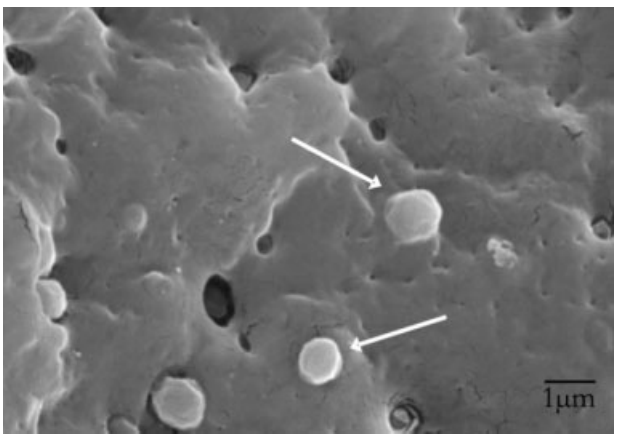

Figure 11 PE in a spherical morphology (white arrows) in the compound PA6/66 GF30 + PE/CB (16 nm).

The batch polymer PA6 only slightly changes the blend's PA6/PA66 ratio. This has no significant effect on morphology or properties in the case of very small variations, as was shown by Nase et al.[1] PE as a third immiscible blend component does decisively change morphology and fracture behavior. It becomes obvious in Figure 11 that PE does appear in a spherical morphology with good adhesion to the polyamide matrix. This PE-based batch is suited to polyamide applications and therefore compatibilized to the chemistry of PA. The PE spheres therefore are responsible for this toughness stabilization that occurs with rising batch concentration.

CONCLUSIONS

CB is the common standard for coloration of polyamide parts. During the development of application-specific polyamide blends and compounds, the composition and especially the influence of the PA6/PA66 ratio, the influence of fiber content and processing aids are comprehensively taken into account to get mechanically resistant and suitable products. This study has shown that, in addition, the apparently simple task of coloring with one CB batch or another has very extensive and significant effects on the mechanical properties of the compounds in general and their resistance against unstable and stable crack propagation in particular.

The use of a finer CB particle as coloring pigment provided a higher compound toughness. The highest stiffness and strength were possible with PA6 as the base of the batch composition in the small diameter CB batches. A greater CB particle diameter leads to a reduction in the resistance against unstable and

stable crack propagation. With increased concentrations of this larger particle, the development of complex CB structures becomes more probable and decreases the resistance against stable crack growth.

Through the introduction of polyethylene as polymer matrix of the batch, it was possible to elevate the toughness in a dry state to a higher level compared to the PA6 based batch. This result was emphasized by the analysis of fracture mechanical properties of the compounds and the identification of well-adhered spherical PE particles by SEM, which provided the highest toughness of dry CB colored compounds.

The influence of CB on mechanical and fracture mechanical properties was comparable in dry and conditioned compounds, which in most cases only differed in the level but not in the trend of their characteristic values.

Mrs. C. Becker and Prof. Dr. G. H. Michler (Martin-Luther-University Halle-Wittenberg) are gratefully acknowledged for the provision of SEM images.

References

1. Nase, M.; Langer, B.; Schumacher, S.; Grellmann, W. J Appl Polym Sci 2009, 111, 2245.
2. Tomova, D.; Radusch, H.-J. Polym Advan Technol 2003, 14, 19.
3. Evstatiev, M.; Schultz, J. M.; Fakirov, S.; Friedrich, K. Polym Eng Sci 2001, 41, 192.
4. Li, Y.; Yang, G. Macromol Rapid Comm 2004, 25, 1714.
5. Li, Y.; Liu, H.; Zhang, Y.; Yang, G. J Appl Polym Sci 2005, 98, 2172.
6. Men, Y.; Rieger, J.; Hong, K. J Polym Sci 2005, 43, 87.
7. Wessling, B. Handbook of Conducting Polymers, Skotheim, T. A.; Elsenbaumer, R. L.; Reynolds, J. R., Eds. Marcel Dekker: New York, 1998; 467.
8. Meinecke, E. A.; Maksin, S. Colloid Polym Sci 1980, 258, 556.
9. King, J. A.; Tucker, K. W.; Vogt, B. D.; Weber, E. H.; Quan, C. Polym Composite 1999, 20, 643.
10. Koszkul, J. Mater Sci 1999, 35, 82.
11. Koysuren, O.; Yesil, S.; Bayram, G. J Appl Polym Sci 2006, 102, 2520.
12. Mucha, M.; Marszalek, J.; Fidrych, A. Polymer 2000, 41, 4137.
13. Mucha, M.; Królikowski, Z. J Therm Anal Calorim 2003, 74, 549.
14. Lafranche, E.; Krawczak, P. Adv Polym Tech 2005, 24, 114.
15. Reincke, K. Ph.D. Dissertation, Martin-Luther-Universität Halle-Wittenberg, 2005.
16. Röthemeyer, F.; Sommer, F. Kautschuktechnologie: Werkstoffe—Verarbeitung—Produkte; Carl Hanser Verlag: München, 2006.
17. Rwei, S.-P.; Ku, F.-H.; Cheng, K.-C. Colloid Polym Sci 2002, 280, 1110.
18. Lim, L.-T.; Britt, I. J.; Tung, M. A. J Appl Polym Sci 1999, 71, 197.
19. Iwatomo, R.; Murase, H. J Polym Sci Pol Phys 2003, 41, 1722.
20. Kawagoe, M.; Nabata, M.; Ishisaka, A. J Mater Sci 2006, 41, 6322.
21. Wan, X. F.; Wang, Y. L.; Zhou, F. G.; Wan, Y. Z. J Reinf Plast Comp 2004, 23, 1031.
22. Ishiaku, U. S.; Hamada, H.; Mizoguchi, M.; Chow, W. S.; Mohd Ishak, Z. A. Polym Compos 2005, 26, 52.
23. Jia, N.; Fraenkel, H. A.; Kagan, V. A. J Reinf Plast Comp 2004, 23, 729.
24. Liou, W. J. J Reinf Plast Comp 1998, 17, 39.
25. Vall'es-Lluch, A.; Camacho, W.; Ribes-Greus, A.; Karlsson, S. J Appl Polym Sci 2002, 85, 2211.
26. Langer, B.; Seidler, S.; Grellmann, W. Deformation and Fracture Behavior of Polymers; Grellmann, W.; Seidler, S., Eds.; Springer Verlag: New York, 2001; p 209.
27. ISO 1110. Plastics—Polyamides—Accelerated conditioning of test specimens, 1995.
28. ISO 1133. Plastics—Determination of the melt mass-flow rate (MFR) and the melt volume-flow rate (MVR) of thermoplastics, 2005.
29. ISO 11357–1. Plastics—Differential scanning calorimetry (DSC)—Part 1: General principles, 1997.
30. ISO 11357–3. Plastics—Differential scanning calorimetry (DSC)—Part 3: Determination of temperature and enthalpy of melting and crystallization, 1999.
31. ISO 6721–1. Plastics—Determination of dynamic mechanical properties—Part 1: General principles, 2001.
32. ISO 527–1. Plastics—Determination of tensile properties—Part 1: General principles, 1993.
33. ISO 527–2. Plastics—Determination of tensile properties—Part 2: Test conditions for moulding and extrusion plastics, 1993.
34. ISO 179–1. Plastics—Determination of Charpy impact properties—Part 1: Non-instrumented impact test, 2000.
35. Grellmann, W.; Seidler, S.; Hesse, W. Deformation and Fracture Behavior of Polymers; Grellmann, W.; Seidler, S., Eds.; Springer-Verlag: New York, 2001; p 71.
36. Grellmann, W.; Seidler, S., Eds. Polymer Testing; Carl Hanser Verlag: München, 2007.
37. Blumenauer, H.; Pusch, G., Eds. Technische Bruchmechanik; Deutscher Verlag für Grundstoffindustrie: Leipzig, 2001.
38. Hornsby, P. R.; Premphet, K. J Mater Sci 1997, 32, 4767.
39. Langer, B.; Bierögel, C.; Kardelky, S.; Mecklenburg, T.; Grellmann, W. In Proceedings of the Polymerwerkstoffe 2002; Halle, September 25–27, 2002; p 476.
40. Mamunya, Y. Mater Sci 2001, 170, 257.